MOLECULAR AND CELLULAR BIOLOGY, Mar. 2011, p. 1160–1173 Vol. 31, No. 6
0270-7306/11/$12.00 doi:10.1128/MCB.00986-10

The Chaperone Network Connected to Human Ribosome-Associated Complex▽‡†

Himjyot Jaiswal,[1,2] Charlotte Conz,[1,3] Hendrik Otto,[1] Tina Wölfle,[1] Edith Fitzke,[1] Matthias P. Mayer,[4] and Sabine Rospert[1,3]*

Institute of Biochemistry and Molecular Biology, ZBMZ, University of Freiburg, Stefan-Meier-Str. 17, D-79104 Freiburg, Germany[1]; Faculty of Biologie, University of Freiburg, Schänzlestr. 1, D-79104 Freiburg, Germany[2]; Centre for Biological Signaling Studies (BIOSS), University of Freiburg, Freiburg, Germany[3]; and Zentrum für Molekulare Biologie der Universität Heidelberg (ZMBH), DKFZ-ZMBH-Allianz, D-69120 Heidelberg, Germany[4]

Received 24 August 2010/Returned for modification 13 October 2010/Accepted 5 January 2011

Mammalian ribosome-associated complex (mRAC), consisting of the J-domain protein MPP11 and the atypical Hsp70 homolog (70-homolog) Hsp70L1, can partly complement the function of RAC, which is the homologous complex from *Saccharomyces cerevisiae*. RAC is the J-domain partner exclusively of the 70-homolog Ssb, which directly and independently of RAC binds to the ribosome. We here show that growth defects due to mRAC depletion in HeLa cells resemble those of yeast strains lacking RAC. Functional conservation, however, did not extend to the 70-homolog partner of mRAC. None of the major human 70-homologs was able to complement the growth defects of yeast strains lacking Ssb or was bound to ribosomes in an Ssb-like manner. Instead, our data suggest that mRAC was a specific partner of human Hsp70 but not of its close homolog Hsc70. On a mechanistic level, ATP binding, but not ATP hydrolysis, by Hsp70L1 affected mRAC's function as a J-domain partner of Hsp70. The combined data indicate that, while functionally conserved, yeast and mammalian cells have evolved distinct solutions to ensure that Hsp70-type chaperones can efficiently assist the biogenesis of newly synthesized polypeptide chains.

Newly synthesized proteins exit the ribosome via a tunnel that traverses the large ribosomal subunit. The tunnel exit is surrounded by a platform consisting of proteins and rRNA, providing the binding sites for dynamically interacting ribosome-bound protein biogenesis factors (RPBs). RPBs serve multiple functions, the most important of which are cotranslational sorting, folding, and covalent modification of newly synthesized polypeptides (22, 36, 53). One of the conserved eukaryotic RPBs is the unusual heterodimeric chaperone complex termed ribosome-associated complex (RAC) in *Saccharomyces cerevisiae* (15) and mammalian ribosome-associated complex (mRAC) in higher eukaryotes (43). RAC and mRAC each consist of a J-domain protein and an Hsp70 homolog (70-homolog) and bind to ribosomes via their J-domain subunit (15, 28, 43, 70). The J-domain subunit of RAC is termed Zuo1, the 70-homolog subunit is termed Ssz1 (15, 70), and the corresponding human subunits are MPP11 and Hsp70L1, respectively (28, 37, 43) (Fig. 1A). In yeast, RAC binds close to Rpl31 at the tunnel exit (45). Binding to Rpl31 is mediated via a charged region within the C-terminal domain of Zuo1 (45, 70). The interaction between Zuo1 and Ssz1 is mediated via the N-terminal domain of Zuo1, preceding the J-domain (10), and requires the peptide binding domain of Ssz1 (6). The N-terminal domain and the charged region are also contained in MPP11, suggesting that their functions are conserved (Fig. 1A). Both RAC and mRAC are stable complexes; the interaction between the two subunits is not affected by the presence of nucleotides. Zuo1 does not serve as the J-domain partner of Ssz1, but the heterodimer as a whole functionally interacts with the 70-homolog Ssb (15, 26), which is encoded by two nearly identical and approximately equally expressed genes termed *SSB1* and *SSB2* (46). Despite evident similarities between RAC and mRAC, there are also significant differences. Ssz1 and Hsp70L1 are distantly related homologs which do not share a greater extent of homology with each other than with canonical Hsp70 homologs. Zuo1 is a 433-amino-acid protein with 35% identity to the N-terminal portion of MPP11. However, MPP11 contains a C-terminal extension and is composed of 621 amino acids. The C-terminal extension of MPP11 contains a two-repeat domain with similarity to the SANT domain family (43, 51, 60) (Fig. 1A). Evolutionary analysis suggests that the SANT-like domain was lost in the fungal branch rather than that it is a more recent acquisition of the mammalian RAC subunit (4). The presence of the SANT-like domain in MPP11 raises a number of questions with respect to functional differences between RAC and mRAC (see Discussion).

RAC stimulates the ATPase activity specifically of Ssb and enhances the interaction of Ssb with newly synthesized polypeptide chains (16, 26, 27). Ssz1 is strictly required for the activity of RAC *in vivo* and *in vitro* but, surprisingly, does not require the peptide binding domain, the ability to hydrolyze ATP, or even binding to ATP (6, 16, 27). The properties of mRAC, and specifically its Hsp70L1 subunit, have not been analyzed until now. Here, we utilized a combination of methods, including knockdown of MPP11 in cell culture, phenotypic

* Corresponding author. Mailing address: Institute of Biochemistry and Molecular Biology, ZBMZ, University of Freiburg, Stefan-Meier-Str. 17, D-79104 Freiburg, Germany. Phone: 49-761-203-5259. Fax: 49-761-203-5257. E-mail: sabine.rospert@biochemie.uni-freiburg.de.

‡ Supplemental material for this article may be found at http://mcb.asm.org/.

▽ Published ahead of print on 18 January 2011.

† The authors have paid a fee to allow immediate free access to this article.

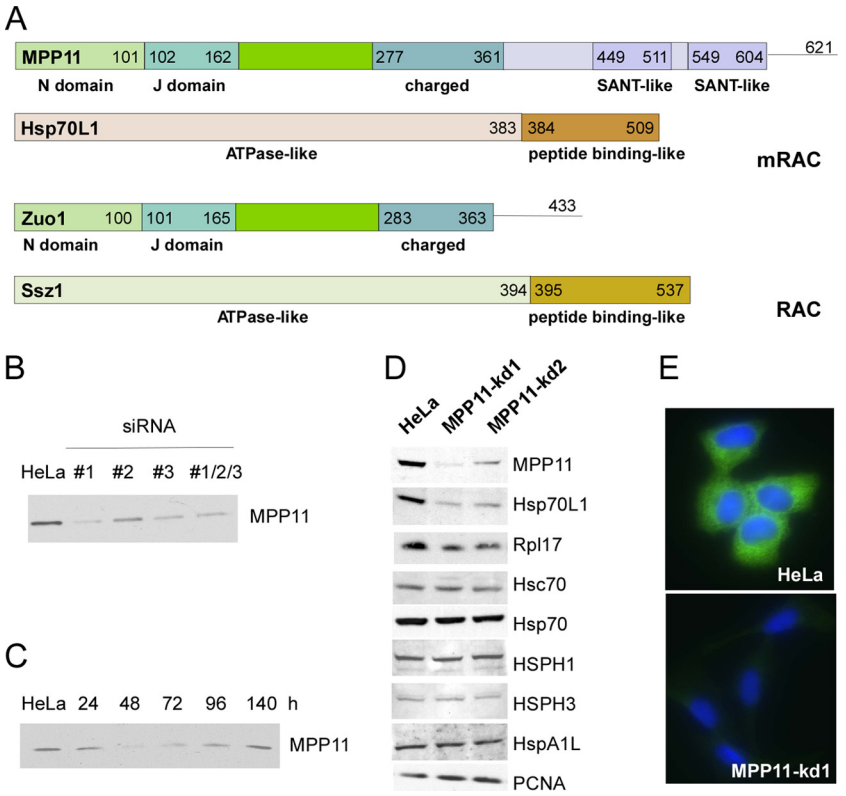

FIG. 1. MPP11 knockdown in HeLa cells. (A) Domain structure of the subunits of heterodimeric mRAC and yeast RAC. mRAC consists of MPP11 and Hsp70L1; RAC consists of Zuo1 and Ssz1. MPP11 and Zuo1 are J-domain proteins, and Hsp70L1 and Ssz1 are 70-homologs. MPP11 and Zuo1 share the N domain (responsible for binding to the respective 70-homolog), the J domain, and the charged region (responsible for binding to the ribosome). MPP11 contains a C-terminal extension with two SANT-like domains of unknown function. For details, see the introduction. (B) MPP11 can be efficiently depleted using siRNA. Aliquots of total lysates containing the same protein concentration from HeLa cells (HeLa) or HeLa cells transiently transfected with one of three different siRNAs directed against MPP11 (#1, #2, and #3) or with a mixture of the three siRNAs were subjected to Western analysis using anti-MPP11. (C) Depletion of MPP11 using siRNA is transient. MPP11 levels in untreated HeLa cells and after 24, 48, 72, 96, and 140 h of transfection with siRNA 1. Cells were harvested at the times indicated, and aliquots of extracts containing the same protein concentration were analyzed via Western blotting using anti-MPP11. (D) Knockdown of MPP11 results in reduced levels of Hsp70L1 and ribosomes. Equal amounts of protein of HeLa cells and of two clones (MPP11-kd1, MPP11-kd2) stably transfected with short hairpin RNA 1 (shRNA 1) were analyzed via Western blotting using antibodies specific for MPP11, Hsp70L1, Rpl17, Hsc70, Hsp70, HSPH1, HSPH3, HspA1L, and the nuclear protein PCNA. (E) Fluorescence microscopic image of HeLa cells and the knockdown cell line MPP11-kd1. Cells were decorated with anti-MPP11 (green), and nuclei are visualized by DAPI (4′,6-diamidino-2-phenylindole) staining (blue).

complementation of yeast deletion strains by mammalian homologs, and functional *in vitro* analysis, to dissect the mechanism of mRAC action. The results identify mRAC as a specific partner of Hsp70, which does not bind to the ribosome directly but is recruited by mRAC. Significant differences between RAC and mRAC, specifically with respect to their 70-homolog partners, indicate general differences in the organizations of the yeast and mammalian Hsp70 networks.

MATERIALS AND METHODS

Constructs and plasmids for expression in mammalian cells. The sequence corresponding to bp 199 to 220 of the MPP11 coding region plus a 9-bp spacer, a HindIII site, and a BglII site was generated by annealing sense (GATCCCGAATTGCAGTTGGAAGAGTTTCAAGAGAACTCTTCCAACTGCAATTCTTTTTGGAAA) and antisense (AGCTTTTCCAAAAAGAATTGCAGTTGGAAGAGTTCTCTTGAAACTCTTCCAACTGCAATTCGG) oligonucleotides and was cloned into the HindIII/BglII sites of the pTER vector (65). The dual-luciferase reporter (DLR) was constructed in the mammalian expression vector pcDNA3.1(+) (Invitrogen). The gene encoding *Renilla* luciferase (r-*LUC*) was amplified from pYDL (21), and the gene encoding firefly luciferase (f-*LUC*) was amplified from pSP-Luc$^+$ (Promega). In the final construct, r-*LUC* is separated from f-*LUC* either by the linker segment AAG CTT GCA GGA ACA CAA **GCA** CAA TTA CAG GAA TTC [in-frame construct pcDNA3.1(+)RLuc-nostop-FLuc] or AAG CTT GCA GGA ACA CAA **TAG** CAA TTA CAG GAA TTC [stop construct pcDNA3.1(+)RLuc-stop-FLuc] as described in reference 48 (boldface indicates differences between sequences).

Plasmids for expression in yeast. Galactose-inducible plasmids for the expression of MPP11 (pESC-flagMPP11), Hsp70L1 (pESC-mycHsp70L1), and mRAC (pESC-flagMPP11-mycHsp70L1) have been described (43). Mutant versions of Hsp70L1 were generated by PCR and were cloned into the pESC-URA3 expression vector (Stratagene), which places them under the control of the *GAL1/GAL10* promoter. Hsp70L1-LKA contains a triple mutation (G200L, T201K, and S202A), and Hsp70L1-K68A and Hsp70L1-E172A contain point mutations in the indicated amino acids. Hsp70L1-ΔC is a C-terminally truncated version of Hsp70L1 that was constructed by placing a stop codon into the coding region of Hsp70L1. The resulting fragment consists of the N-terminal 383 amino acids of Hsp70L1. The fragment of Hsp70L1 is homologous to the ATPase domain fragment of Hsc70 (amino acids 1 to 387), of which the X-ray structure was solved (12) (see Table 2; also see Fig. S1 in the supplemental material). The human 70-homologs (Table 1) were amplified from the following cDNA clones: Hsp70 (HSP70A1A/B), Deutsches Ressourcenzentrum für Genomforschung (RZPD) accession no. NM_005345; HspA1L, RZPD accession no. NM_005527; HspA2, OriGene accession no. NM_021979; HspA6, RZPD accession no. NM_002155; HspA12B, OriGene accession no. NM_052970; Hsc70 (HspA8),

TABLE 1. Human 70-homologs employed for complementation in yeast strains lacking Ssa, Ssb, Sse1, and Ssz1[a]

Hsp70 family	Gene/protein name(s)	Alternative name	Size of protein (kDa)	Comments	Reference(s)
HSP A	HSPA8	**Hsc70**	71	Isoform 1 (amino acids 1–646), major, constitutively expressed homolog in the human cytosol	7, 20, 61, 64
		Hsc54	53	Isoform 2 (amino acids 1–493)	64
	HSPA1A, HSPA1B	**Hsp70**	70	Identical, depending on the tissue, constitutively expressed or stress induced	7, 20, 61
	HSPA14	**Hsp70L1**	55	Complex partner of MPP11, ribosome-associated	43
	HSPA1L	Hsp70-Hom	70		13
	HSPA2	HspA2	70		20
	HSPA6	HspA6	71		20
	HSPA12B	HspA12B	76		20
HSP H	HSPH1	HspH1/Hsp105	97		31
	HSPH2	HspA4/Apg2	94		20
	HSPH3	HspA4L/Apg1	95		20

[a] The gene/protein names are according to the nomenclature introduced in references 20 and 33). The alternative name is a synonym commonly used (5). We have used the alternative names in this study. The homologs which were purified and used for *in vitro* experiments are indicated in bold. References for the cytosolic location do not exclude the possibility that the homologs are also found at other locations, e.g., the nucleus. In some cases, the localization of the homolog has only been predicted and not experimentally verified.

RZPD accession no. NM_006597; HSPH1 (Hsp105), OriGene accession no. NM_006644; HSPH2 (Hsp4A/Agp2), OriGene accession no. NM_002154; and HSPH3 (HspA4L/Apg1), OriGene accession no. NM_014278. Hsc54 is a truncated version of Hsc70 comprised of amino acids 1 to 463 and was constructed by PCR based on Hsc70. Each homolog was cloned in frame with the plasmid-encoded N-terminal myc tag into the galactose-inducible yeast expression vector pESC-HIS3 (Stratagene). Expression in yeast was tested using a myc tag antibody (see Fig. S2A to C in the supplemental material). The coding regions of all plasmids were sequenced in order to ensure that no other mutations were present. The expression level of the MPP11 constructs was tested by immunoblotting using anti-FLAG antibodies (see Fig. S3A and B in the supplemental material).

Plasmids for expression in *Escherichia coli*. Constructs for expression of an N-terminally His_6-tagged version of proteins in *E. coli* are based on pET28a or pACYC-Duet1, which are suited for coexpression of proteins in *E. coli* (Novagen). Hsp70 and Hsc70 were amplified from cDNA clones (RZPD accession no. NM_005345 and NM_006597) and were cloned into the NdeI/BamHI or NheI/SalI sites of pET28a, resulting in plasmids pET28a-his-HspA1A and pET28a-Hsc70, respectively. Using PCR technology, AAG coding for lysine at position 71 of Hsp70 was exchanged for GCG coding for alanine, resulting in pET28a-his-HspA1A-K71A. The purified proteins are termed Hsp70, Hsc70, and Hsp70-K71A. Hsp70L1 and MPP11 were cut with NcoI/BamHI from pET28a-hisHsp70L1 or pET28a-hisMPP11, respectively (43) and were cloned into pACYC-Duet1 cut with NcoI/BglII, resulting in pACYC-Duet1-hisHsp70L1 and pACYC-Duet1-hisMPP11. The coding sequences of Hsp70L1-K68A, Hsp70L1-E172A, and Hsp70L1-LKA were amplified from pESC-mycHsp70L1-K68A, pESC-mycHsp70L1-E172A, and pESC-mycHsp70L1-LKA and were cloned into NdeI/BamHI site of pET28a, resulting in plasmids pET28a-hisHsp70L1-K68A, pET28a-hisHsp70L1-E172A, and pET28a-hisHsp70L1-LKA. pET28a-hisMPP11-QPD was generated by replacing a SacII/KpnI fragment within the coding region of MPP11 in pET28a-hisMPP11 (43) with the corresponding SacII/KpnI fragment amplified from pESC-flagMPP11-QPD-mycHsp70L1. For the purification of mRAC complexes containing wild-type MPP11, pACYC-Duet1-hisMPP11 was coexpressed with pET28a-hisHsp70L1 (mRAC), pET28a-hisHsp70L1-K68A (mRAC-K68A), pET28a-hisHsp70L1-E172A (mRAC-E172A), or pET28a-hisHsp70L1-LKA (mRAC-LKA). To obtain mRAC-QPD, hisHsp70L1 and MPP11-QPD were coexpressed from plasmids pACYC-Duet1-hisHsp70L1 and pET28a-hisMPP11-QPD.

Yeast media and culture conditions. Standard yeast genetic techniques were applied (59). Strains were grown to log phase in medium containing 2% peptone, 1% yeast extract, and either 2% dextrose (YPD) or 2% galactose (YPGal). Growth defects were analyzed by spotting 10-fold serial dilutions of cultures containing the same number of cells onto YPD or YPGal plates. Plates were incubated at 30°C to analyze the slow-growth phenotype and at 20°C to test for cold sensitivity. Sensitivity to paromomycin was analyzed on plates supplemented with paromomycin at the concentrations specified in the figure legends.

Yeast strains. MH2723f**a**/α (*ura3*/*ura3 leu2*/*leu2 his3*/*his3 trp1*/*trp1 ade2*/*ade2*) (24) is the parental wild-type strain of all haploid derivatives used in this study. The Δ*zuo1* Δ*ssz1* (Ida12 *zuo1*::*TRP1 ssz1*::*LEU2*) (15) and Δ*ssb1* Δ*ssb2* (Ida56E: *ssb1*::*ADE2 ssb2*::*ADE2*) deletion strains were previously described (6). The Δ*zuo1* Δ*ssz1* Δ*ssb1* Δ*ssb2* (Ida1256E *zuo1*::*TRP1 ssz1*::*LEU2 ssb1*::*ADE2 ssb2*::*ADE2*) quadruple-deletion strain was generated by mating Ida12 with Ida56E, followed by sporulation and tetrad analysis. Deletion of Zuo1, Ssz1, and Ssb was confirmed by Western blotting (see Fig. S3 in the supplemental material; also data not shown). To generate the Δ*zuo1* Δ*ssz1* Δ*sse1* strain, *SSE1* plus 300 bp up- and downstream of the open reading frame (ORF) was cloned into pSP65 (Promega) and an internal Tth111I/BglII fragment was replaced by the *HIS3* marker gene. The *sse1*::*HIS3* fragment was introduced into the Ida12 strain, resulting in Ida12Kai1 (*zuo1*::*TRP1 ssz1*::*LEU2 sse1*::*HIS3*).

The Δ*ssa1* Δ*ssa2* Δ*ssa3* Δ*ssa4* (Δ*ssa1-4*) pYCPlac33-SSA1 strain was generated using the *loxP-kanMX-loxP* gene disruption cassette (19). For this purpose, *SSA1* to *-4* each and 300 bp up- and downstream of the ORF sequence were cloned into pSP65. In plasmids pSP65-SSA1, pSP65-SSA2, and pSP65-SSA3, an internal fragment of the respective genes (*SSA2*, KpnI/SexAI; *SSA3*, BclI/BamHI; *SSA4*, AgeI/BglII) was replaced by the *loxP-kanMX-loxP* cassette amplified from pUG6 (19). In the case of *SSA1*, a KpnI/SexAI fragment was replaced with the *TRP1* marker gene. The *SSA4*::*lox-kanMX-lox* disruption construct was amplified by PCR and was transformed in parallel into the haploid **a** and α MH2723f strains. Next, the *URA3*-based pSH47 plasmid containing cre recombinase under the control of a galactose-inducible promoter was transformed. After induction on galactose, cells were selected for loss of the *loxP-kanMX-loxP* locus by replica plating the cells in the absence and presence of G418. Clones which had lost G418 resistance were cured from the pSH47 plasmid by growth on 5-fluoro uracil (5-FOA). The procedure was repeated for *SSA3* and *SSA2*. The resulting haploid Δ*ssa2* Δ*ssa3* Δ*ssa4* α strain was transformed with a *TRP1* plasmid and the corresponding Δ*ssa4* Δ*ssa3* Δ*ssa2* **a** strain with a URA3 plasmid, and the two strains were mated. The diploid (*ssa2*/*ssa2 ssa3*/*ssa3 ssa4*/*ssa4*) strain, which had lost the *TRP1* and *URA3* plasmid after prolonged growth on medium containing tryptophan and uracil was selected and was transformed with the *ssa1*::*TRP1* deletion cassette fragment. The resulting strain (*ssa1*/*SSA1 ssa2*/*ssa2 ssa3*/*ssa3 ssa4*/*ssa4*) was transformed with plasmid pYCPlac33-Ssa1 and was subsequently sporulated. Tetrad dissection and analysis of the haploid spores generated the Δ*ssa1*Δ*ssa2* Δ*ssa3* Δ*ssa4* pYCPlac33-SSA1 (*ssa1*::*TRP1* Δ*ssa2* Δ*ssa3* Δ*ssa4* pYCPlac33-SSA1) strain. As expected, quadruple-deletion strains lacking plasmid-borne *SSA1* were inviable.

Cell culture, transfection, and generation of stable knockdown cell lines. HeLa cells were from the American Type Culture Collection (ATCC) and maintained in Dulbecco's modified Eagle's medium (DMEM) (Sigma-Aldrich) containing 10% fetal bovine serum (Gibco). Transfections of plasmids and small interfering RNA (siRNA) (siRNA 1, bp 197 to 217; siRNA 2, bp 989 to bp 1009; and siRNA 3, bp 1609 to 1629 of the MPP11 coding sequence) was performed by the calcium phosphate method (55). Stable pTER cell lines were generated as described previously using pTER-shRNA1 (65). Zeocin-resistant clones (MPP11-kd cell lines) were tested for their ability to downregulate MPP11 by Western blotting and via immunofluorescence (43) using anti-MPP11.

Cell proliferation. Equal numbers of cells of the HeLa, MPP11-kd1, or MPP11-kd2 line were plated in 6-cm petri dishes with or without G418 (Gibco) or NaCl at the concentrations indicated in the figure legends. After the times indicated, cells were trypsinized and counted at three different dilutions using a Neubauer hemocytometer. The results for MPP11-kd2 (data not shown) were similar to those for MPP11-kd1. The sensitivity of HeLa and MPP11-kd1 cells to amphotericin B was tested as described previously (25, 35). In brief, 4×10^5 cells were grown for 24 h, were washed successively with 2 ml of phosphate-buffered saline (PBS) and 2 ml of medium, and were then incubated for 1 h at 37°C with 2 ml medium containing amphotericin B at the concentrations indicated in the figure legends. The medium was removed and cells were washed with 2 ml of PBS, detached using 200 μl of trypsin, and finally incubated with 0.4% trypan blue solution. Viable cells which had not incorporated the dye were counted.

Cell extract preparation for Western blotting. Total yeast extracts were prepared as described previously (69). HeLa cell extracts for immunoblotting were prepared as described previously (68). In brief, HeLa cells were trypsinized, collected, and then incubated for 15 min in 50 mM HEPES-KOH, pH 7.4, 80 mM K acetate, 1 mM Mg acetate, 1 mM phenylmethylsulfonyl fluoride (PMSF), 1× protease inhibitor cocktail (PIC) (1,000× PIC is 1.25 mg/ml leupeptin, 0.75 mg/ml antipain, 0.25 mg/ml chymostatin, 0.25 mg/ml elastatinal, and 5 mg/ml pepstatin A dissolved in dimethyl sulfoxide [DMSO]), and 0.5% Triton X-100 at 4°C. Lysed cells were centrifuged for 20 min at 20,000 × *g* at 4°C, and the supernatant was used for further experiments. Protein concentrations were determined with the bicinchoninic acid (BCA) assay (Sigma-Aldrich) according to the manufacturer's instructions, using bovine serum albumin (BSA) as a standard.

Ribosome profiles. Ribosome profiles were determined as described previously (43), with the exception that cell lysis was performed by vortexing in the presence of glass beads. To that end, 50- to 70%-confluent HeLa cells were incubated with 100 μg/ml cycloheximide for 1 h, trypsinized, collected, and resuspended in 2× the volume of the cell pellet lysis buffer (50 mM HEPES-KOH, pH 7.4, 1 mM Mg acetate, 1 mM PMSF, 1× PIC). Approximately 1× the volume of the cell pellet of glass beads was added, and cell disruption was performed by vortexing the cells six times for 20 s at 4°C, followed by a 40-s interval on ice and then by a clarifying spin at 2,500 × *g* for 10 min. Ten units of optical density at 260 nm (OD_{260}) of HeLa cell extract in lysis buffer containing either 80 mM K acetate, 80 mM K acetate-2 mM ATP, or 80 mM K acetate-0.25 mg/ml RNase A was loaded on a linear 15%-to-55% sucrose gradient. After centrifugation at 200,000 × *g* (model TH641 centrifuge; Sorvall Instruments) for 2.5 h at 4°C, gradients were fractionated from top to bottom with a density gradient fractionator monitoring A_{254} (Teledyne ISCO) (43, 49). The fractions and a total corresponding to 1/20 of the material loaded onto the sucrose gradient were analyzed via immunoblotting using the antibodies indicated in the figure legends. To quantify the effect of MPP11 depletion on the binding of Hsc70 and Hsp70 to translating ribosomes, aliquots of polysome fractions derived from HeLa and MPP11-kd1 cell extracts were run on Tris-Tricine gels (56) and were subsequently analyzed via Western blotting using exposures in the linear range for Hsp70, Hsc70, and Rpl17. The intensities of the bands were determined desitometrically (AIDA image analyzer; raytest). Note that polysome fractions of HeLa and MPP11-kd1, used for the individual quantifications, were loaded onto a single gel. The sum of the intensities of Hsp70 or Hsc70 bands was then divided by the sum of the intensities of the corresponding Rpl17 bands. The ratio between Hsp70 or Hsc70 and Rpl17 in HeLa polysome fractions was set as 100%. The respective values determined for the MPP11-kd1 polysome fractions were expressed as percentages of the HeLa values.

Purification of proteins expressed in *E. coli*. Bag1 was purified as described previously (14). Hsp70, Hsc70, and mRAC were expressed at high levels and were soluble in *E. coli* (data not shown). Extracts were prepared via sonication of induced cells resuspended in a buffer containing 40 mM HEPES-KOH, 240 mM K acetate, 5 mM Mg acetate, and 15 mM imidazole, pH 7.4. After centrifugation at 17,000 × *g* at 4°C for 30 min, the pH of the supernatant was adjusted to 7.8 and was applied to a purification step via Ni-nitrilotriacetic acid (NTA) (Qiagen) according to the manufacturer's protocol for native-protein purification. The material eluted from the Ni beads was dialyzed against 2 liters of 10 mM potassium phosphate buffer, pH 7.4, at 4°C overnight and was loaded onto an 8-ml hydroxyapatite column (ceramic hydroxyapatite; Bio-Rad). Bound proteins were eluted with a 25-ml, 0 to 300 mM linear gradient of potassium phosphate buffer, pH 7.4. Hsp70 eluted at a concentration of 50 to 240 mM potassium phosphate. Hsp70-containing fractions were pooled and loaded onto a MonoQ HR5/5 anion-exchange column (GE Healthcare). Elution of bound proteins was performed with a 70 to 700 mM, 18-ml linear potassium acetate gradient in 40 mM HEPES-KOH, pH 7.4. Hsp70 eluted at a concentration of 70 to 450 mM K acetate. Fractions containing Hsp70 were pooled, and the buffer was exchanged with 40 mM HEPES-KOH, 240 mM K acetate, 10% glycerol, pH 7.4, using Vivaspin 4 columns (Sartorius). Purification of Hsp70-K71A and Hsc70 was performed by applying the same protocol except for the Ni-NTA purification step, which in the case of the Hsc70 purification was performed in potassium phosphate buffer, pH 7.4. Preparations containing 4 to 8 mg of purified Hsp70, Hsp70-K71A, or Hsc70 were frozen in liquid nitrogen and stored at −80°C. See Fig. 5A and 6B for purified proteins and complexes.

MPP11 and the mRAC versions were purified after induction of *E. coli* cells harboring the appropriate expression plasmids (see above). Cell lysis and Ni-NTA purification were as described above in a buffer containing 40 mM potassium phosphate, 240 mM KCl, and 15 mM imidazole, pH 7.8. The material eluted from Ni-NTA was diluted to a final concentration of 10 mM potassium phosphate, was loaded onto an 8-ml hydroxyl apatite column (ceramic hydroxyapatite; Bio-Rad), and was eluted with a 25-ml linear gradient of 200 to 500 mM potassium phosphate, pH 7.8. MPP11 eluted at a concentration of 240 to 380 mM potassium phosphate, and mRAC eluted at 250 to 320 mM potassium phosphate. MPP11- or mRAC-containing fractions were pooled, were diluted to a final concentration of 50 mM potassium phosphate, were loaded onto a MonoQ HR5/5 anion-exchange column (GE Healthcare), and were eluted with 22 ml of a 90 to 600 mM linear K acetate gradient in 40 mM HEPES-KOH, pH 7.8. MPP11 was recovered in the flowthrough of the MonoQ column, while mRAC eluted at 280 to 400 mM K acetate. For further purification, MPP11 was directly loaded on a Mono S HR5/5 cation-exchange column (GE Healthcare). In the case of mRAC, fractions were pooled and diluted with 40 mM HEPES-KOH buffer (pH 7.8) to a final concentration of 50 mM K acetate before being loaded onto Mono S. MPP11 and mRAC were eluted with an 80 to 800 mM K acetate linear gradient in 40 mM HEPES-KOH, pH 7.8. MPP11 eluted at a K acetate concentration of 330 to 690 mM, whereas mRAC eluted at 260 to 290 mM. Purified MPP11 and mRAC preparations were concentrated to 1 to 10 mg/ml in 40 mM HEPES-KOH (pH 7.8)–240 mM K acetate as described above, were supplemented with 10% glycerol, and were stored at −80°C. Purification of the mRAC variants was performed using the same protocol. Purification of yeast RAC and RAC-LKA was performed as described previously (6).

Nucleotide dissociation. ADP dissociation was performed as described previously (14) using the fluorescent ADP analogues N8-(4*N*′-methylanthraniloylaminobutyl)-8 aminoadenosine 5′-diphosphate (MABA-ADP) (62) and a stopped-flow device (SX-18 M; Applied Photophysics, Surrey, United Kingdom). Hsp70 (0.5 μM) was preincubated for 30 min with 0.5 μM MABA-ADP in HKM buffer (25 mM HEPES-KOH, pH 7.6, 50 mM KCl, 5 mM $MgCl_2$) and mixed 1:1 with a solution containing 100 μM ATP in the absence or presence of 5 μM mRAC in HKM buffer at 30°C.

Determination of ATP hydrolysis rates. Steady-state ATPase assays were carried out at 30°C as described previously (6, 26). In brief, reactions of 50 μl contained 100 μM ATP, 0.037 MBq of [α-^{32}P]ATP, 20 mM HEPES-KOH, pH 7.4, 120 mM K acetate, 5 mM Mg acetate. The ATP hydrolysis was monitored by thin-layer chromatography, and the rate of ATP hydrolysis was calculated by linear fitting of the data.

***In vivo* readthrough assays.** Readthrough assays were performed as described previously (21, 48) with HeLa cells or MPP11-kd cells transfected with pcDNA3.1(+)RLuc-nostop-FLuc or pcDNA3.1(+)RLuc-stop-FLuc. Cells were harvested and assayed for firefly and *Renilla* luciferase activities 48 h after transfection using the dual-luciferase reporter (DLR) assay system according to the protocol of the manufacturer (Promega). With this assay system, firefly and *Renilla* luciferases are measured sequentially in a single reaction. Luciferase activities are given in relative light units (RLU). The efficiency of the readthrough was determined based on the ratio between firefly luciferase (f-Luc) activity and *Renilla* luciferase (r-Luc) activity. The f-Luc/r-Luc activity ratio was set to 100% when the enzymes were expressed at equimolar quantities from the in-frame RLuc-nostop-FLuc construct. The efficiency of readthrough is expressed as the percentage of the f-Luc/r-Luc activity ratio obtained with the RLuc-stop-FLuc construct. Normalization with the RLuc-nostop-FLuc was performed independently for the wild-type and MPP11-kd cell lines.

Miscellaneous. Western blots were developed using enhanced chemiluminescence (ECL) as described previously (49). Photo-cross-linking to [α-^{32}P]8-azido-ATP or [α-^{32}P]8-azido-ADP was as described previously (6, 26). Quantification of Western blots and thin-layer chromatographs was performed using the AIDA image analyzer (raytest). Anti-MPP11, -Hsp70L1, -hRPL17, -HspA1L, -HspH1, and -HSPH3 are polyclonal antibodies directed against peptides of the respective proteins (Eurogentec). Anti-mouse IgG–horseradish peroxidase (HRP), anti-rabbit IgG–Alexa 488, anti-mouse IgG–fluorescein isothiocyanate (FITC) (Sigma), anti-rabbit IgG–HRP (Pierce), anti-Hsc70 (Abcam), anti-Hsp70 (Biomeda), anti-PCNA (BD Bioscience), anti-FLAG (Novagen), and anti-myc (Chemicon) were also used.

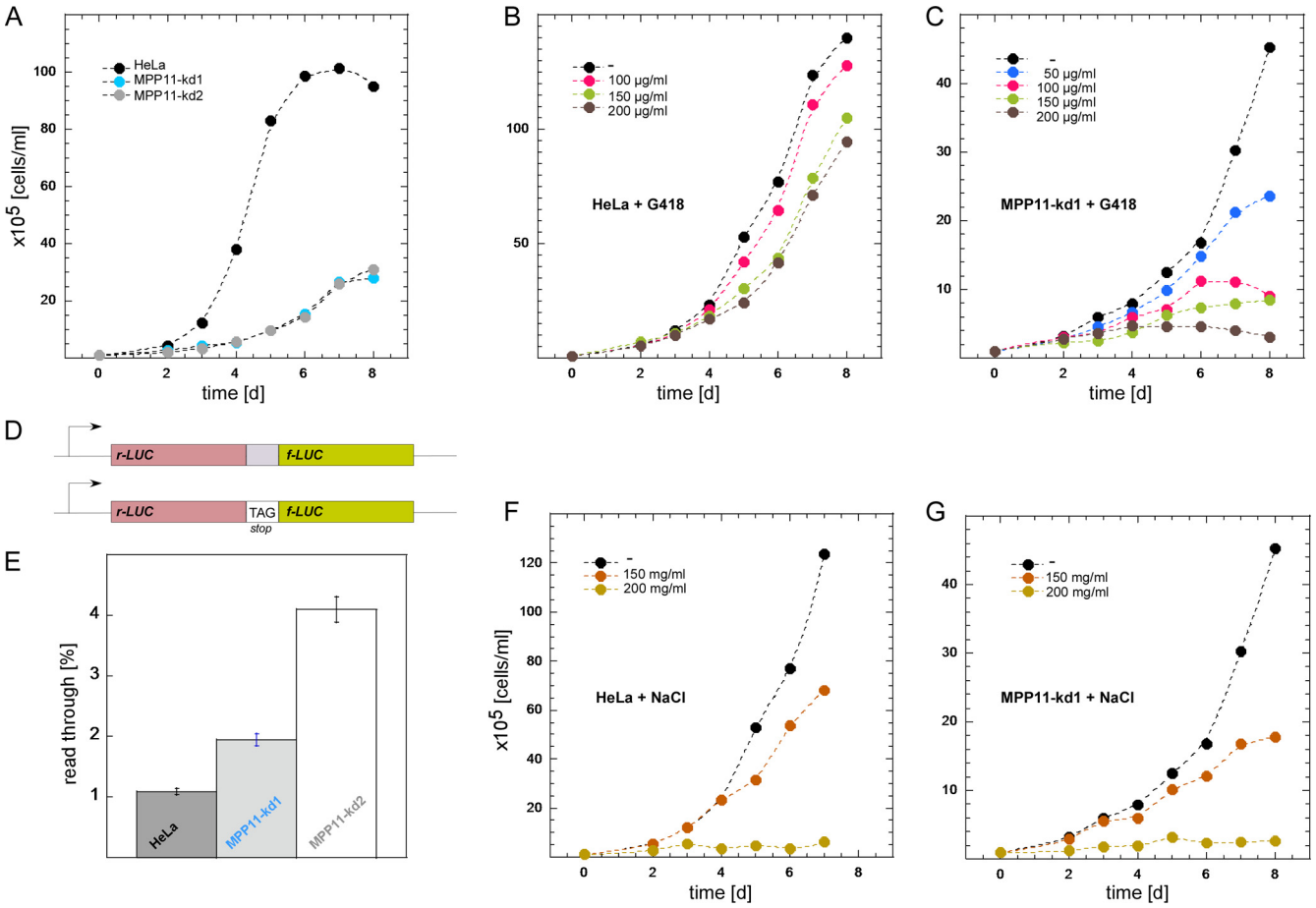

FIG. 2. Phenotypic effects of the MPP11 knockdown. (A) MPP11 knockdown results in slow growth and sensitivity to the aminoglycoside G418. HeLa, MPP11-kd1, or MPP11-kd2 cells were grown for the indicated times at 37°C. HeLa cells (B) or MPP11-kd1 cells (C) were grown in the absence (−) or in the presence of the indicated amounts of the aminoglycoside G418. (D) Readthrough reporter constructs. Dual reporter consisting of firefly luciferase (f-Luc) and *Renilla* luciferase (r-Luc) separated by either an in-frame short linker or a linker containing the TAG stop codon (*stop*). (E) Readthrough of a stop codon is enhanced in MPP11-kd cells. The readthrough efficiency through the TAG stop codon was determined 48 h after transient transfection of HeLa, MPP11-kd1, and MPP11-kd2 cells. f-Luc and r-Luc activities were determined for the in-frame and stop constructs, and readthrough efficiencies were calculated as described in Materials and Methods. HeLa cells (F) or MPP11-kd1 cells (G) were grown in the absence (−) or in the presence of the indicated concentrations of NaCl. d, days.

RESULTS

Effects of MPP11 depletion in mammalian cells. To better understand the function of human MPP11, we have investigated the effect of MPP11 depletion in HeLa cells. Initially, transient knockdowns of MPP11 using three different siRNA constructs were performed. All three siRNAs resulted in a significant reduction of MPP11 at the protein level (Fig. 1B). A time course revealed that the knockdown was most efficient 48 to 72 h after transfection (Fig. 1C). The sequence of siRNA 1 was chosen to generate a stable knockdown of MPP11 in HeLa cells. Three independent clones were isolated and tested for MPP11 depletion (Fig. 1D and E). In all cases, MPP11 was significantly reduced (Fig. 1D, lanes MPP11-kd1 and MPP11-kd2, and data not shown). Moreover, the steady-state level of Hsp70L1 was reduced in the MPP11-kd cell lines, indicating that Hsp70L1 was destabilized in the absence of its partner subunit MPP11 (Fig. 1D). The expression levels of the cytosolic 70-homologs Hsc70, Hsp70, HSPH1, HSPH3, and HspA1L were not affected by MPP11 depletion (Fig. 1D). As indicated by the decreased steady-state level of the ribosomal protein Rpl17, MPP11-kd cells contained a reduced level of ribosomes compared to HeLa cells (Fig. 1D).

The knockdown of MPP11 resulted in pronounced slow growth (Fig. 2A) and in hypersensitivity toward the aminoglycoside G418 (compare Fig. 2B and C; also data not shown). Aminoglycosides bind to ribosomes close to the decoding center and enhance the rate of translational errors. In many cases, mutants which suffer from a decrease in translational fidelity are hypersensitive to this class of drugs (11, 54). To test if MPP11 indeed affects the fidelity of translation, a dual-reporter construct consisting of *Renilla* luciferase (r-Luc) and firefly luciferase (f-Luc) was generated. The two genes were separated either by an in-frame linker or by a linker containing the TAG stop codon (Fig. 2D). Translation of the in-frame construct gives rise to a fusion protein, which exhibits both r-Luc and f-Luc activities. Translation of the stop construct results in the production of only r-Luc. Only if readthrough occurs will the fusion protein be generated. In HeLa cells, the

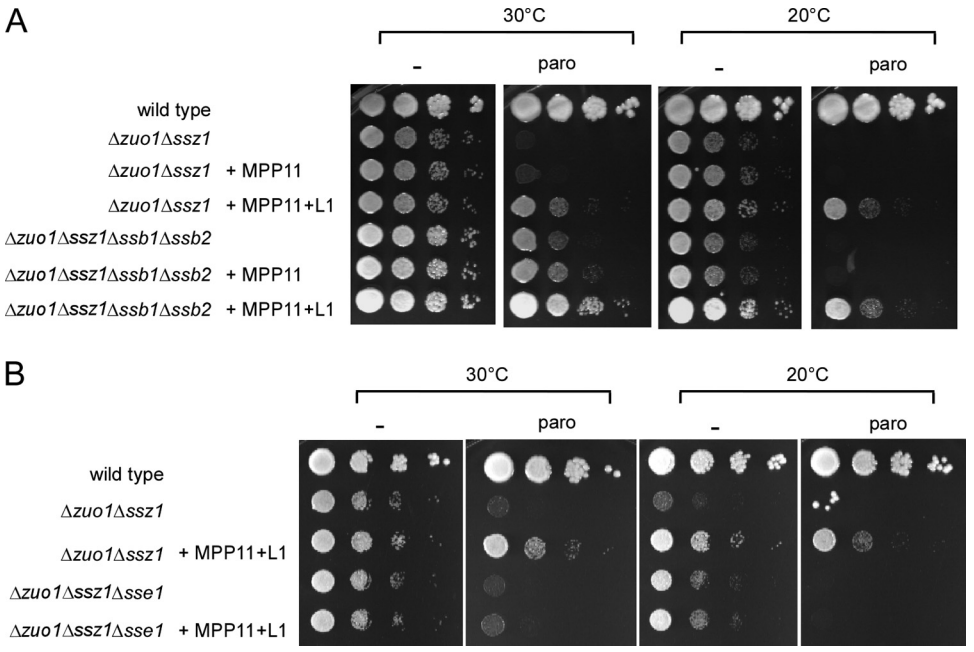

FIG. 3. Complementation of the Δ*zuo1* Δ*ssz1* strain by MPP11 or mRAC does not require Ssb but does require Sse1. MPP11, Hsp70L1, or both proteins were expressed under the control of the GAL promoter in the yeast strains, as indicated. Serial 10-fold dilutions of galactose-grown cultures containing equal numbers of cells were spotted onto YPGal plates containing 20 μg/ml paromomycin (paro) where indicated and were incubated for 3 days at 30°C and for 6 days at 20°C. (A) Complementation by mRAC is more efficient than complementation by MPP11 and does not require Ssb. (B) Complementation of the Δ*zuo1* Δ*ssz1* strain by mRAC requires Sse1.

stop codon readthrough occurred with a frequency of about 1%. The frequency was significantly enhanced for both MPP11-kd1 and MPP11-kd2 (Fig. 2E); the differences between the two knockdown cell lines most likely reflect integration-specific effects.

Increased readthrough upon depletion of MPP11 closely resembled the situation in Δ*zuo1* and Δ*ssb1* Δ*ssb2* strains (48). Based on experimental evidence, it was suggested that in yeast, a major cause of the aminoglycoside sensitivity observed in Δ*zuo1* and Δ*ssb1* Δ*ssb2* strains is an increase in the membrane potential, resulting in enhanced uptake of toxic cations, as, for example, with aminoglycosides and Na^+ (34, 46, 53). We thus tested if MPP11-kd cells displayed enhanced sensitivity toward NaCl. In contrast to the corresponding yeast mutants, HeLa and MPP11-kd cells displayed similar sensitivities to NaCl; growth was partly inhibited by the addition of 150 mg/ml NaCl, while both cell lines were unable to grow in the presence of 200 mg/ml NaCl (compare Fig. 2F and G, and data not shown). Thus, the loss of MPP11 did not result in a general sensitivity toward cations. MPP11-kd cells were also not sensitive toward amphotericin B (see Fig. S4 in the supplemental material), a drug that inhibits the growth of HeLa cells by disrupting membrane integrity (25, 35). How exactly the specific toxicity of aminoglycosides is influenced by mRAC/RAC is currently not understood (46, 53). Interestingly, increased sensitivity toward this class of drugs has also been observed in yeast mutants lacking ribosomal proteins localized at the exit of the ribosomal tunnel (9, 45). One possibility is that translational fidelity can be affected by ribosomal proteins and ribosome-bound factors at the tunnel exit via the nascent polypeptide chain or via allosterically transmitted conformational changes within the ribosome.

Identification of mRAC partners. Previous studies have shown that MPP11 by itself weakly complements the growth defects of a Δ*zuo1* Δ*ssz1* strain (28, 43). Complementation is significantly enhanced if MPP11 and Hsp70L1 are coexpressed and the heterodimeric mRAC complex can form (43) (Fig. 3A). Complementation by MPP11 is independent of Ssb (28); however, whether or not complementation by mRAC is dependent on or independent of Ssb has previously not been tested. Because Zuo1 strictly requires Ssz1 to cooperate with Ssb (16, 26), it seemed possible that MPP11 strictly requires Hsp70L1 to function with Ssb. To that end, MPP11 or mRAC was expressed in a Δ*zuo1* Δ*ssz1* or a Δ*zuo1* Δ*ssz1* Δ*ssb1* Δ*ssb2* background (Fig. 3A; also see Fig. S3A and B in the supplemental material). Neither MPP11 nor mRAC required Ssb for complementation of the Δ*zuo1* Δ*ssz1* strain, indicating that not only MPP11 but also mRAC did not cooperate with Ssb. None of the mammalian 70-homologs is closely related to Ssb, and it has been speculated that Ssb-type 70-homologs are confined to fungi (47). To test this hypothesis directly, we expressed N-terminally myc-tagged versions of 11 human cytosolic 70-homologs (Table 1 and data not shown; see also Fig. S2A in the supplemental material) for their ability to complement the growth defects of a Δ*ssb1* Δ*ssb2* strain. Note that the expression levels of the 11 human 70-homologs differed to some extend, most likely reflecting different levels of stability in the yeast cytosol. However, the major cytosolic 70-homologs Hsp70 and Hsc70, as well as Hsc54, Hsp70-Hom, and HspA2, were expressed at high, comparable levels that were detectable

even in Ponceau S stains (see Fig. S2 in the supplemental material; also data not shown). As a result, none of the human 70-homologs significantly enhanced the growth of the Δ*ssb1* Δ*ssb2* strain (Fig. 4A).

The combined data suggested that the partner of mRAC in yeast was Ssa, the second major 70-homolog of the yeast cytosol. Ssa, encoded by the close homologs *SSA1* to *-4*, is essential, and it is not straightforward to test if Ssa is required for mRAC function *in vivo*. However, Sse1 is a nonessential nucleotide exchange factor which acts in concert with Ssa and Ssb (46). Because complementation of the Δ*zuo1* Δ*ssz1* strain by mRAC was Ssb independent (Fig. 3A), a requirement for Sse1 would provide strong evidence for an Ssa/Sse1-dependent mechanism of mRAC function. Indeed, when mRAC was expressed in a Δ*zuo1* Δ*ssz1* Δ*sse1* background, its ability to complement was lost (Fig. 3B; also see Fig. S2C in the supplemental material), indicating that Sse1 is required for mRAC function. The most straightforward explanation for this observation is that mRAC acts as a heterologous J-domain partner of Ssa but that Sse1 is required as a nucleotide exchange factor for Ssa in this system.

To investigate directly which of the 70-homologs (Table 1) was functionally related to Ssa, we generated a yeast strain in which all four copies of *SSA* were deleted by a pop-in pop-out approach (Δ*ssa1-4* strain). The strain was rescued by expression of *SSA1* from a URA3 plasmid. In this strain background, the mammalian 70-homologs (Table 1) were expressed from a HIS3 plasmid (Fig. 4B; also see Fig. S2B in the supplemental material). As a control, a HIS3 plasmid containing *SSA1* was included in the analysis. After the strains were cured from the URA3 plasmids, only strains containing the HIS3 plasmid bearing *SSA1* or the Hsc70 gene were viable (Fig. 4C). Thus, Hsc70, but no other 70-homolog, was able to complement the lethal phenotype of a Δ*ssa1-4* strain. The possibility cannot be excluded that mammalian 70-homologs, for example, HspA6, which was consistently expressed at a relatively low level (Table 1; also see Fig. S2), failed to complement for that reason.

mRAC can act as a J-domain partner of Hsp70 and Hsc70 *in vitro*. Using purified components (Fig. 5A and 6B), we aimed to answer two basic questions. First, how restrictive is mRAC with respect to its partner 70-homolog? To address this question, we examined the interplay between mRAC and Hsp70/Hsc70. Second, how does the Hsp70L1 subunit affect the function of MPP11 as a J-domain protein? To that end, we generated and analyzed a set of mutants in the Hsp70L1 subunit of the mRAC complex.

To test the effect of mRAC on possible 70-partners, we expressed and purified mRAC, Hsp70, Hsc70, and Bag1 from *E. coli* (Fig. 5A). Hsp70 and Hsc70 are 85% identical; however, they display different kinetic properties. The k_{cat} of purified Hsp70 was 0.05 min^{-1}, while the k_{cat} of Hsc70 was 0.29 min^{-1} (Fig. 5C, D, and E). The data are consistent with those from a previous study in which untagged Hsp70 and Hsc70 were compared (14). The N-terminal His tag thus did not affect the kinetic properties of Hsp70 or Hsc70. Purified mRAC stimulated the ATPase activity of Hsp70 in substoichiometric amounts and in a concentration-dependent manner (Fig. 5B). When a 4-fold excess of mRAC was applied, the rate of ATP hydrolysis was stimulated approximately 6-fold (Fig. 5B, C, and E). ATP hydrolysis by Hsc70 was also stimulated in the presence of a 4-fold excess of mRAC but only 1.4-fold (Fig. 5D and E). The stimulation of Hsp70's and Hsc70's ATPase activities by mRAC was similar to that previously reported for the J-domain protein Hdj1 (14). The presence of the nucleotide exchange factor Bag1 further enhanced the rate of ATP hydrolysis by Hsp70 and Hsp70 (Fig. 5C, D, and E). The data suggest that mRAC is a bona fide J-domain partner of Hsp70 as well as of Hsc70.

ATP binding to Hsp70L1 is essential for complementation of the Δ*zuo1* Δ*ssz1* strain by mRAC. We generated a set of mutations within Hsp70L1 (Table 2; see Fig. S1 in the supplemental material). The effects of the different Hsp70L1 mutations were tested in the Δ*zuo1* Δ*ssz1* strain, which coexpresses MPP11. As a control, the J-domain mutant MPP11-QPD was coexpressed with Hsp70L1 (Fig. 6A; see Fig. S3B in the supplemental material). This mutation in the J-domain of MPP11 abolishes the ability of mRAC to complement growth defects in yeast (28, 43).

Two mutations in Hsp70L1, L1-E172A and L1-K68A (see Fig. S1 in the supplemental material), were designed to abolish any potentially existing, low ATPase activity of Hsp70L1 (41, 67). L1-LKA was designed according to a previously characterized triple mutation within the ATPase domain of Ssz1, which disturbs γ-phosphate coordination and abolishes ATP binding (6) (see Fig. S1 and S5 in the supplemental material). Finally, a mutant lacking the peptide binding domain, termed L1-ΔC, was generated. As reported for the corresponding yeast mutant (6), L1-ΔC failed to form a complex with MPP11 (see Fig. S3C in the supplemental material). MPP11 in combination with L1-E172A, L1-K68A, or L1-ΔC suppressed the growth defects of the Δ*zuo1* Δ*ssz1* strain as efficiently as wild-type Hsp70L1 (Fig. 6A). Thus, similarly to what was previously shown for the corresponding yeast mutants (6), neither ATPase activity nor the stable interaction of Hsp70L1 with MPP11 was required for complementation in yeast. However, unlike with the yeast system (6), L1-LKA had entirely lost the ability to complement in the presence of MPP11 (Fig. 6A). To test if loss of function of L1-LKA correlated with a defect in nucleotide binding, we subjected purified mRAC complexes to UV-induced cross-linking in the presence of α-^{32}P-labeled 8-azido-ATP or 8-azido-ADP (6, 26) (Fig. 6B). Note that the preparations contained identical nucleotide concentrations with the same specific radioactivity, and cross-linking experiments with the two nucleotide analogs were performed in parallel. The relative affinities of 8-azido-ATP and 8-azido-ADP in the experiments can thus be compared directly. Wild-type Hsp70L1 was cross-linked to 8-azido-ATP quite efficiently (Fig. 6B and C). The efficiency of 8-azido-ATP cross-linking to the catalytic site mutants L1-K68A and L1-E172A was enhanced. However, L1-LKA displayed only very low cross-linking to 8-azido-ATP, indicating that the mutant displayed a strong defect in ATP binding (Fig. 6B and C). We consistently observed a moderate enhancement of 8-azido-ADP cross-linking to L1-LKA (Fig. 6B and C). This finding indicates not only that the L1-LKA mutant assembled into the mRAC complex in yeast (see Fig. S3C) and *E. coli* (Fig. 6B) but also that the general structure of the L1-LKA nucleotide binding pocket was preserved. We also observed that 8-azido-ADP was cross-linked to the MPP11 subunit of the mRAC complex but that this was not the case for 8-azido-ATP (Fig. 6B). While the significance of this observation is not clear, it might be related

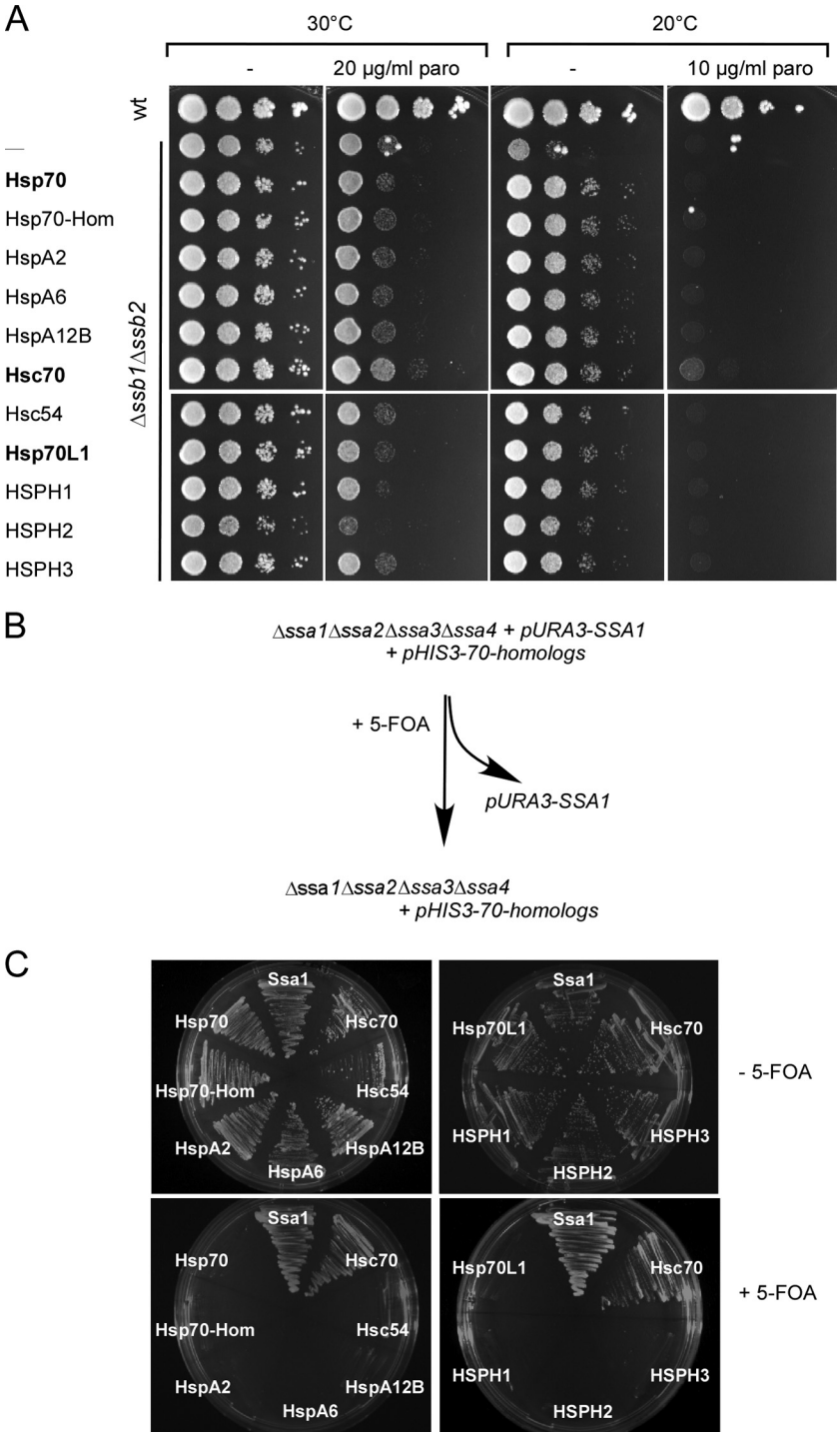

FIG. 4. Complementation of the yeast Δ*ssb1* Δ*ssb2* and Δ*ssa1-4* strains by human 70-homologs. (A) Human 70-homologs do not complement the growth defects of the Δ*ssb1* Δ*ssb2* strain. Complementation was tested as described in the legend of Fig. 3 on YPGal plates containing the indicated paromomycin concentrations. Plates were incubated for 3 days at 30°C and for 6 days at 20°C. See also Fig. S2A in the supplemental material. wt, wild type. (B) Experimental setup for the identification of human 70-homologs with the ability to complement the lethal phenotype of a Δ*ssa1* Δ*ssa2* Δ*ssa3* Δ*ssa4* strain. (C) Only Hsc70 was able to rescue the lethal phenotype of the Δ*ssa1-4* strain. Strains expressing pURA3-SSA1 and different pHIS3-Hsp70-homologs were plated on 5-FOA-containing plates and were incubated for 3 days at 30°C. See also Fig. S2B in the supplemental material.

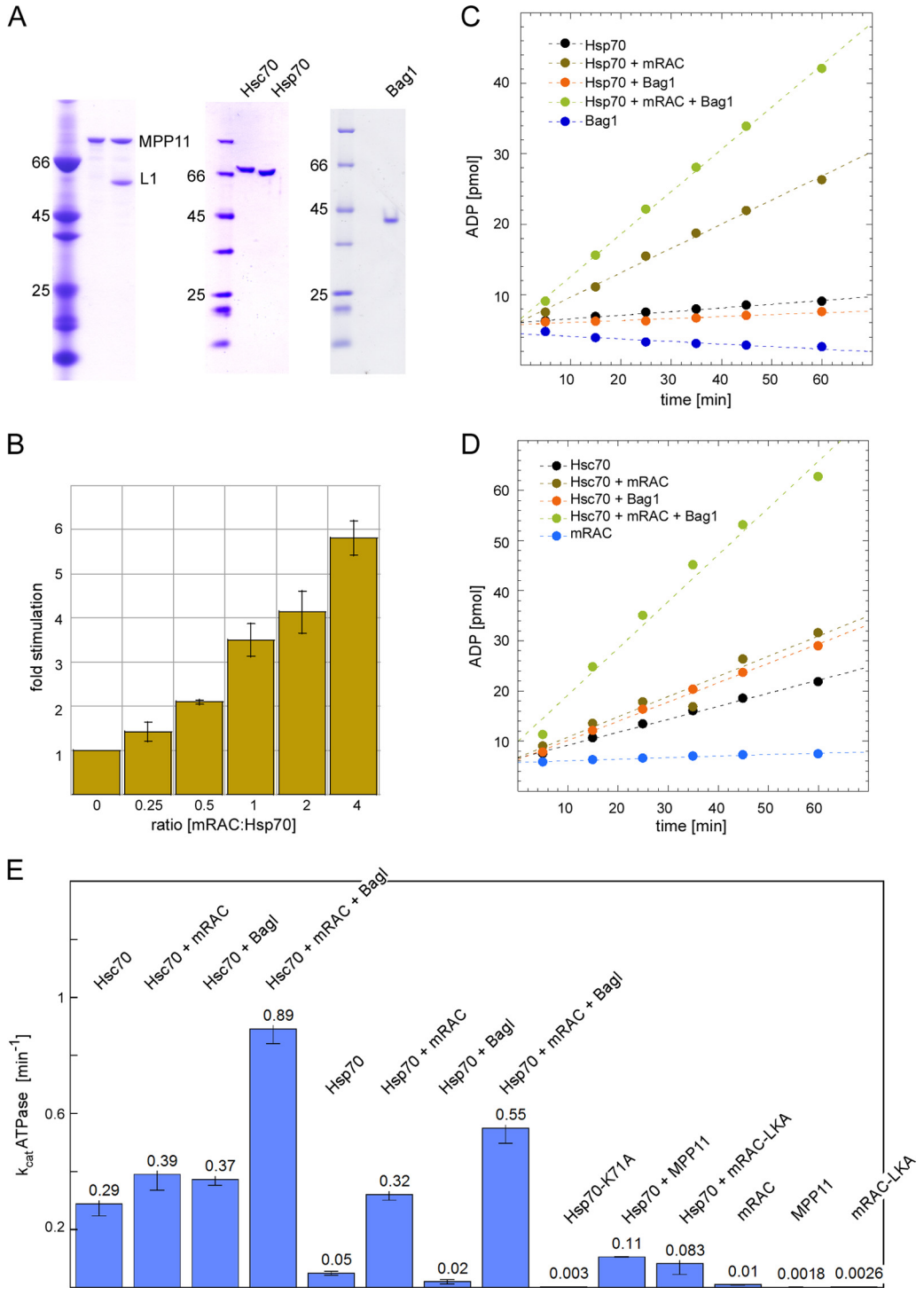

FIG. 5. mRAC stimulates the ATPase activity of Hsp70 and Hsc70. (A) Purified MPP11 (2 μg), mRAC (2 μg), Hsp70 (2 μg), Hsc70 (2 μg), and Bag1 (1 μg). Proteins were subjected to SDS-PAGE and were analyzed by staining with Coomassie blue. (B) mRAC stimulates Hsp70 in a concentration-dependent manner. The steady-state activity of Hsp70 was determined in the presence of 100 μM ATP at 30°C (Materials and Methods). The rate of ATP hydrolysis was determined at increasing mRAC concentrations and was normalized to the rate of ATP hydrolysis in the absence of mRAC. (C and D) mRAC stimulates Hsp70 and Hsc70. Steady-state activities of Hsp70 (0.5 μM) (C) or Hsc70 (0.5 μM) (D) were determined in the presence of 100 μM ATP at 30°C (see Materials and Methods). Reactions were performed in the absence or presence of Bag1 (0.5 μM) or mRAC (2 μM) as indicated. (E) Stimulation of Hsc70 and Hsp70 by mRAC, mutant versions of mRAC, and Bag1. Steady-state activities were determined at 30°C in the presence of 100 μM ATP. The concentration of Hsc70 or Hsp70 in the reaction mixture was 0.5 μM. Mutant versions of mRAC were applied in a 4-fold molar excess above the concentration of Hsc70 or Hsp70. Bag1 was applied in equimolar amounts. Experiments were performed at least three times, with the exception of the experiment for Hsp70-K71A, whose stimulation was determined only once. The mean of the k_{cat} is indicated on top of each bar. Error bars indicate standard deviations.

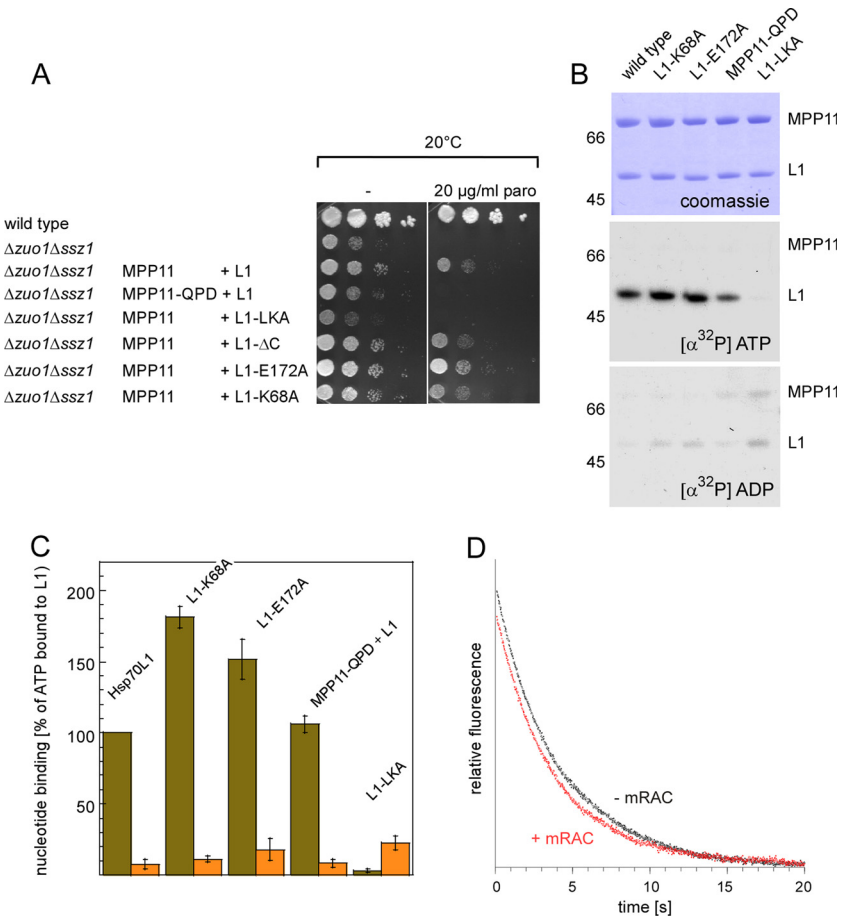

FIG. 6. Modulation of MPP11 by Hsp70L1 depends on ATP binding. (A) Complementation of growth defects of the Δ*zuo1* Δ*ssz1* strain by mRAC depends on the ability of Hsp70L1 to bind to ATP. Δ*zuo1* Δ*ssz1* strains expressing MPP11 plus either Hsp70L1 (L1), L1-E172A, L1-K68A, L1-LKA, or L1-ΔC (Table 2) were analyzed as described for Fig. 3. (B) Mutations in Hsp70L1 affect binding to nucleotides. (Upper panel) Coomassie stain of 2.5-μg purified mRAC complexes. (Lower panels) Autoradiography of purified mRAC complexes cross-linked to either [α-^{32}P]8-azido-ATP or [α-^{32}P]8-azido-ADP. The nucleotide analogs contained the same specific radioactivity, and the autoradiographs were exposed for the same length of time. (C) Efficiency of nucleotide cross-linking to the different L1 versions. After cross-linking of the indicated wild-type and mutant mRAC complexes to either [α-^{32}P]8-azido-ATP (olive columns) or [α-^{32}P]8-azido-ADP (orange columns), samples were analyzed as shown in panel B. The α-^{32}P-labeled signals were normalized with respect to the corresponding Coomassie blue-stained protein band, and the amount of 8-azido-ATP, which was cross-linked to wild-type Hsp70L1, was set to 100%. Error bars indicate the standard deviations derived from at least 3 data sets. (D) mRAC does not enhance the rate of nucleotide exchange on Hsp70. MABA-ADP was prebound to Hsp70, and the rate of dissociation was determined in the presence or absence of a 10-fold molar excess of mRAC as described in Materials and Methods.

to MPP11's C-terminal SANT domain, because Zuo1 of the RAC complex was not cross-linked to 8-azido-ADP (see Fig. S5). In contrast to Hsp70L1 (Fig. 6B and C), Ssz1 cross-linked with similar efficiencies to both nucleotide analogs (see Fig. S5).

TABLE 2. Mutations within the mRAC subunits[a]

mRAC subunit	Name	Mutation(s)
MPP11	MPP11-QPD	H119Q (inactivation of the J domain)
Hsp70L1	L1-K68A	K68A (inactivation of the ATPase)
	L1-E172A	E172A (inactivation of the ATPase)
	L1-LKA	G200L, T201K, S202A (affects γ-phosphate coordination)
	L1-ΔC	Amino acids 1–383 (deletion of the C-terminal domain)

[a] See Fig. 1A; also see Fig. S1 in the supplemental material.

ATP binding to Hsp70L1 affects the function of mRAC as a cochaperone. The yeast system strictly depends on Ssz1 not only *in vivo* but also *in vitro*: RAC effectively stimulates the ATPase of Ssb, but Zuo1 by itself is basically inactive (26). In contrast to what occurs in the yeast system, MPP11 stimulated the ATPase of Hsp70; however, mRAC was more effective (Fig. 5E; see Fig. S6 in the supplemental material). Interestingly, MPP11 by itself and mRAC-LKA displayed very similar stimulations of ATP hydrolysis by Hsp70 (Fig. 5E; see Fig. S6). Thus, the inability of mRAC-LKA to rescue the growth defect of a Δ*zuo1* Δ*ssz1* strain (Fig. 6A) correlated with a defect of mRAC-LKA to stimulate Hsp70 (Fig. 5E; see Fig. S6). The combined data demonstrate that the function of mRAC depends on ATP binding to Hsp70L1 but does not depend on ATP hydrolysis. Similar properties have been reported for the 70-homolog Sse1, which acts as a nucleotide exchange factor for Ssa (see also above) and, to that end, requires ATP binding

but does not require ATPase activity (57, 58). The similarity suggested to us that mRAC might act not only as a J-domain partner but also as a nucleotide exchange factor for Hsp70. To test this, the effect of mRAC on the dissociation of the fluorescently labeled ADP analogue MABA-ADP prebound to Hsp70 was measured in stopped-flow experiments. Dissociation of MABA-ADP from Hsp70 was not affected by mRAC (Fig. 6D). We conclude that Hsp70L1 within the mRAC complex did not serve as a nucleotide exchange factor for Hsp70.

Hsp70L1 may hydrolyze ATP, albeit slowly. Hsp70 in general possesses very low intrinsic ATPase activities. The ability of a 70-homolog to be stimulated by cochaperones or substrate proteins confirms that it is a bona fide ATPase (38). In default of a stimulating partner for Hsp70L1, we compared the steady-state activities of mRAC, mRAC-LKA, and MPP11 (Fig. 5E). As a result, the k_{cat} of mRAC was significantly higher than that of mRAC-LKA or MPP11. However, the rate of ATP hydrolysis was only 0.01 ATP per min, which is very close to background hydrolysis. Based on the currently available data, the question of whether Hsp70L1 can hydrolyze ATP cannot be conclusively answered. However, at least the function of Hsp70L1 in yeast does not depend on its ability to hydrolyze ATP (Fig. 6A).

mRAC enhances the interaction of Hsp70 with nascent chains in mammalian cells. Ssb interacts with ribosomes independently of whether or not RAC is present and independently of whether or not ribosomes are translating (48, 49). However, the interaction of Ssb with the nascent chain requires the presence of functional RAC (16). Moreover, other 70-homologs, which do not directly interact with the ribosome, can be recruited to nascent chains by specific J-domain partners. For example, overexpression of the ribosome-associated J-domain protein Jjj1, which functions in concert with Ssa but not Ssb, allows Ssa to partially substitute for the RAC/Ssb system (39). Hsp70 and Hsc70 do not directly bind to the ribosome but interact transiently and in an ATP-dependent way with the ribosome-bound nascent chain (see Fig. S7A in the supplemental material) (2, 63). Thus, the question arose as to whether there was a requirement for J-domain partners to target Hsp70 and Hsc70 to nascent chains. To test for this possibility, the ability of mRAC, which is not released from ribosomes upon ATP treatment (see Fig. S7A in the supplemental material), to target the major 70-homologs Hsp70 and Hsc70 to translating ribosomes was tested. To that end, the Hsp70 and Hsc70 contents of polysome profiles were tested using specific antibodies (see Fig. S7B). A side-by-side analysis revealed that significantly less Hsp70 was bound to polysomes of MPP11-kd1 than to HeLa cells (Fig. 7A to C). However, binding of Hsc70 to polysomes remained unaffected whether or not mRAC was present (Fig. 7A to C). Thus, mRAC was involved in the recruitment specifically of Hsp70 to nascent chains.

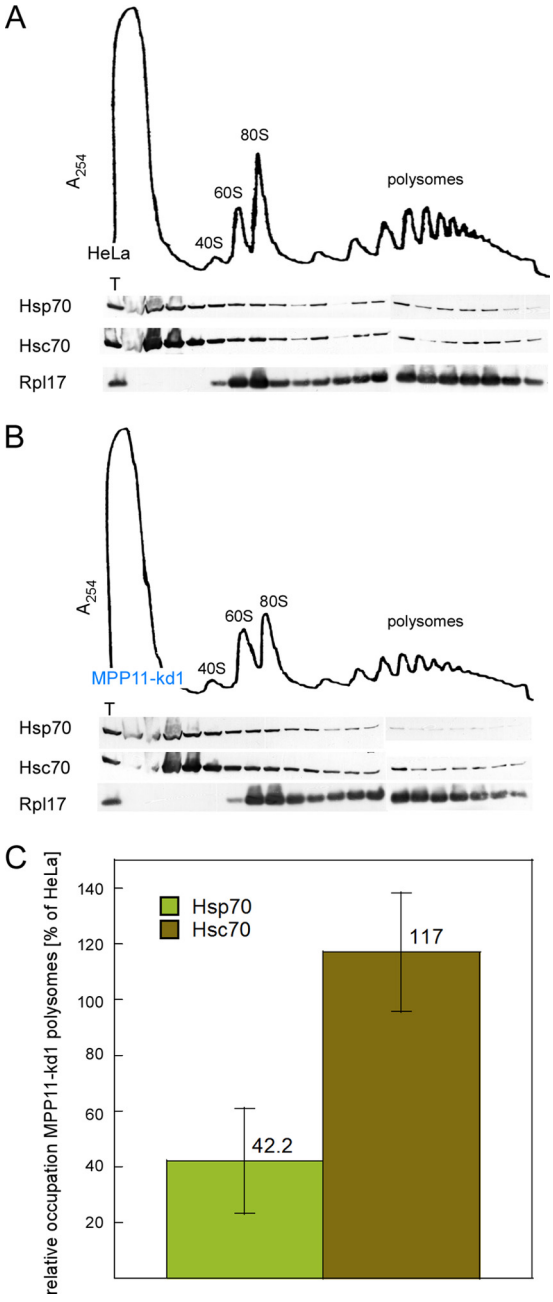

FIG. 7. mRAC enhances binding of Hsp70, but not Hsc70, to nascent chains. Ribosome profiles of HeLa and MPP11-kd1 cell extracts were performed as described in Materials and Methods. Polysome profiles of HeLa cell extract (A) and MPP11-kd1 cell extract (B) were run in parallel and were analyzed for the distribution of Hsp70, Hsc70, and ribosomes (Rpl17). (C) Polysome fractions of HeLa or MPP11-kd1 profiles as shown in panels A and B were analyzed for their relative contents of Rpl17, Hsp70, and Hsc70 via Western blotting as described in Materials and Methods. The ratio of Hsp70 to Rpl17 or Hsc70 to Rpl17 in HeLa cells was set as 100%. Error bars indicate the standard deviations derived from the results of at least 3 independent experiments.

DISCUSSION

Ssb, which is directly anchored to the ribosome and, with the assistance of RAC (16), interacts with emerging polypeptide chains, is the paradigm of cotranslational chaperone function in eukaryotic cells (22, 36, 46). While this setup seems to fit the requirements of cotranslational protein folding perfectly, it is confined to fungi. In mammalian cells, only mRAC is anchored to the ribosome. At least the major 70-homologs Hsc70 and Hsp70 do not bind to the ribosome directly but interact with translating ribosomes via the nascent polypeptide (2, 63) (see Fig. S7A in the supplemental material). It has been previously

reported that Hsc70 and Hsp70 possess distinct kinetic properties, despite the fact that they are close homologs (14). Our results confirm this observation and, moreover, identify two additional functional differences. First, Hsc70, but not Hsp70, was able to complement Ssa in yeast. Second, Hsp70, but not Hsc70, required mRAC to be efficiently recruited to ribosome-bound nascent chains in mammalian cells. While details explaining the distinct behaviors are currently not understood, the results suggest that Hsp70 may function together with mRAC, similarly to the Ssb-RAC system, directly at the tunnel exit. The recruitment of Hsp70 to that location may be achieved by its enhanced rate of ATP hydrolysis in close proximity to mRAC. Stimulation of the ATPase might be specifically important in the case of Hsp70, because the intrinsic hydrolysis rate of this 70-homolog is low (Fig. 5E). Alternatively, mRAC may directly bind to nascent chains, either by its MPP11 or Hsp70L1 subunit, and hand the nascent chain over specifically to Hsp70.

We found that recruitment of Hsc70 to translating ribosomes was independent of mRAC. One possibility is that Hsc70 was able to interact with nascent chains independently of mRAC, because it possesses significantly higher intrinsic ATPase activity (Fig. 5E) (14). ATP hydrolysis triggers the closing of the substrate binding cavity and the locking-in of associated substrates (38). Alternatively, additional J-domain proteins in the mammalian cytosol may be involved in the recruitment of Hsc70 to nascent chains. Independently of what determines the functional differences between Hsp70 and Hsc70, the combined data suggest that the two 70-homologs serve distinct functions rather than represent two interchangeable, abundant, multipurpose chaperones which differ only in their means of transcriptional regulation (5, 32).

We have tested the functional overlap between human and yeast 70-homologs in the case of not only Ssa (Fig. 4C) but also Ssb (Fig. 4A), Sse1 (see Fig. S2D in the supplemental material), and Ssz1 (6; data not shown). The results demonstrate a surprisingly clear-cut partitioning between the yeast and mammalian Hsp70 systems. Not a single mammalian 70-homolog was able to complement the growth defects of the Δ*ssb1* Δ*ssb2* or Δ*sse1* strain. Exclusively, Hsp70L1, which remarkably shares only 28% identity with Ssz1, partly complemented the defects of a Δ*ssz1* strain (43). What might be the reason for the low compatibility between the yeast and mammalian systems? One possible explanation is that cochaperones like J-domain proteins, nucleotide exchange factors, or partner 70-homologs fail to intermingle between lower and higher eukaryotes. Alternatively, the promiscuity of 70-homologs with respect to their client proteins might be less pronounced than is generally anticipated.

Besides compelling phenotypic similarities caused by the loss of mRAC and RAC in their respective cellular backgrounds, there are significant differences, and our data suggest that these relate to the specificities of the respective mammalian and yeast chaperone networks as a whole. The major open question with respect to MPP11 relates to the function of its SANT domains. SANT domains are found in chromatin-remodeling complexes and interact with histone tails or DNA (3). Interestingly, GlsA, the MPP11 homolog from *Volvox*, interacts with histones via its SANT domains (44). The loss of GlsA causes, besides defects in asymmetric cell division, cold sensitivity as well as sensitivity to aminoglycosides in *Volvox* (44). A GlsA variant lacking the SANT domain was able to rescue cold sensitivity and aminoglycoside sensitivity; however, the SANT domain was essential for asymmetric cell division (44). In this respect, it is also interesting that mammalian MPP11, yeast Zuo1, and the *Caenorhabditis elegans* homolog DNJ-11 localize predominantly to the cytosol (23, 28, 43) but that the bulk of GlsA localizes to the nucleus (40). Recently, it was found that MPP11, termed ZRF1 (zuotin-related factor 1) in that study, affects transcriptional activation during differentiation by affecting histone H2A deubiquitination (52). A role for MPP11 and its homologs in chromatin remodeling is consistent with a number of reports that connect MPP11, or its homologs, to transcriptional regulation (29, 30, 71), cancer progression (17, 18, 42, 51), and asymmetric cell division (23, 40, 44). Whether Hsp70L1 also functions in these seemingly ribosome-unrelated processes is currently not understood, and the role of Hsp70L1 in the mRAC complex is not well defined. Our data indicate that Hsp70L1 is not a nucleotide exchange factor, a function more recently discovered for a subclass of 70-homologs (8, 50). However, the role of Hsp70L1 requires its ability to bind to ATP. This property allows for a regulatory mechanism connecting the activity of mRAC, and in turn the activity of ribosome-bound Hsp70, to the cellular ATP concentration. If the level of ATP is high, mRAC is active; if the level drops, e.g., upon a sudden energy shortage, mRAC is inactivated. In the case of Ssz1, such a mechanism does not seem to apply, because ATP binding is dispensable for Ssz1's *in vivo* function (6). However, in yeast, Ssb is special not only because it binds to ribosomes directly but also because it possesses an unusually high K_m, which allows for direct regulation via the cellular ATP concentration (46). A model in which the activities of chaperones directly coupled to the translational machinery are regulated by the energy status of the cell is an attractive possibility. Translation in yeast is shut down within minutes when cells are depleted from the energy source glucose (1), and this process has recently been shown to require the presence of Ssb (66). Future investigations will aim at elucidating the roles of the ribosome-bound chaperones in regulating the coupling between transcription, translation, and subsequent steps of protein biogenesis.

ACKNOWLEDGMENTS

This work was supported by grants SFB 746 and Forschergruppe 967 and by the Excellence Initiative of the German Federal and State Governments (grant EXC 294) (to S.R.).

Plasmids pTER and pYDL were generous gifts from H. Clevers and D. Dinman.

REFERENCES

1. **Ashe, M. P., S. K. De Long, and A. B. Sachs.** 2000. Glucose depletion rapidly inhibits translation initiation in yeast. Mol. Biol. Cell **11:**833–848.
2. **Beckmann, R. P., L. A. Mizzen, and W. J. Welch.** 1990. Interaction of hsp70 with newly synthesized proteins: implications for protein folding and assembly. Science **248:**850–854.
3. **Boyer, L. A., R. R. Latek, and C. L. Peterson.** 2004. The SANT domain: a unique histone-tail-binding module? Nat. Rev. Mol. Cell Biol. **5:**158–163.
4. **Braun, E. L., and E. Grotewold.** 2001. Fungal Zuotin proteins evolved from MIDA1-like factors by lineage-specific loss of MYB domains. Mol. Biol. Evol. **18:**1401–1412.
5. **Brocchieri, L., E. Conway de Macario, and A. J. Macario.** 2008. hsp70 genes in the human genome: conservation and differentiation patterns predict a wide array of overlapping and specialized functions. BMC Evol. Biol. **8:**19.
6. **Conz, C., et al.** 2007. Functional characterization of the atypical Hsp70 subunit of yeast ribosome-associated complex. J. Biol. Chem. **282:**33977–33984.

7. **Cvoro, A., A. Korac, and G. Matic.** 2004. Intracellular localization of constitutive and inducible heat shock protein 70 in rat liver after in vivo heat stress. Mol. Cell. Biochem. **265:**27–35.
8. **Dragovic, Z., S. A. Broadley, Y. Shomura, A. Bracher, and F. U. Hartl.** 2006. Molecular chaperones of the Hsp110 family act as nucleotide exchange factors of Hsp70s. EMBO J. **25:**2519–2528.
9. **Dresios, J., I. L. Derkatch, S. W. Liebman, and D. Synetos.** 2000. Yeast ribosomal protein L24 affects the kinetics of protein synthesis and ribosomal protein L39 improves translational accuracy, while mutants lacking both remain viable. Biochemistry **39:**7236–7244.
10. **Fiaux, J., et al.** 2009. Structural analysis of the ribosome-associated complex RAC reveals an unusual Hsp70/Hsp40 interaction. J. Biol. Chem. **285:**3227–3234.
11. **Fischel-Ghodsian, N.** 1999. Genetic factors in aminoglycoside toxicity. Ann. N. Y. Acad. Sci. **884:**99–109.
12. **Flaherty, K. M., C. DeLuca-Flaherty, and D. B. McKay.** 1990. Three-dimensional structure of the ATPase fragment of a 70K heat-shock cognate protein. Nature **346:**623–628.
13. **Fourie, A. M., P. A. Peterson, and Y. Yang.** 2001. Characterization and regulation of the major histocompatibility complex-encoded proteins Hsp70-Hom and Hsp70-1/2. Cell Stress Chaperones **6:**282–295.
14. **Gässler, C. S., T. Wiederkehr, D. Brehmer, B. Bukau, and M. P. Mayer.** 2001. Bag-1M accelerates nucleotide release for human Hsc70 and Hsp70 and can act concentration-dependent as positive and negative cofactor. J. Biol. Chem. **276:**32538–32544.
15. **Gautschi, M., et al.** 2001. RAC, a stable ribosome-associated complex in yeast formed by the DnaK-DnaJ homologs Ssz1p and zuotin. Proc. Natl. Acad. Sci. U. S. A. **98:**3762–3767.
16. **Gautschi, M., A. Mun, S. Ross, and S. Rospert.** 2002. A functional chaperone triad on the yeast ribosome. Proc. Natl. Acad. Sci. U. S. A. **99:**4209–4214.
17. **Greiner, J., et al.** 2003. Characterization of several leukemia-associated antigens inducing humoral immune responses in acute and chronic myeloid leukemia. Int. J. Cancer **106:**224–231.
18. **Greiner, J., et al.** 2004. mRNA expression of leukemia-associated antigens in patients with acute myeloid leukemia for the development of specific immunotherapies. Int. J. Cancer **108:**704–711.
19. **Güldener, U., S. Heck, T. Fielder, J. Beinhauer, and J. H. Hegemann.** 1996. A new efficient gene disruption cassette for repeated use in budding yeast. Nucleic Acids Res. **24:**2519–2524.
20. **Hageman, J., and H. H. Kampinga.** 2009. Computational analysis of the human HSPH/HSPA/DNAJ family and cloning of a human HSPH/HSPA/DNAJ expression library. Cell Stress Chaperones **14:**1–21.
21. **Harger, J. W., and J. D. Dinman.** 2003. An in vivo dual-luciferase assay system for studying translational recoding in the yeast Saccharomyces cerevisiae. RNA **9:**1019–1024.
22. **Hartl, F. U., and M. Hayer-Hartl.** 2009. Converging concepts of protein folding in vitro and in vivo. Nat. Struct. Mol. Biol. **16:**574–581.
23. **Hatzold, J., and B. Conradt.** 2008. Control of apoptosis by asymmetric cell division. PLoS Biol. **6:**e84.
24. **Heitman, J., N. R. Movva, P. C. Hiestand, and M. N. Hall.** 1991. FK 506-binding protein proline rotamase is a target for the immunosuppressive agent FK 506 in Saccharomyces cerevisiae. Proc. Natl. Acad. Sci. U. S. A. **88:**1948–1952.
25. **Hidaka, K., S. I. Akiyama, and M. Kuwano.** 1981. Amphotericin B resistance is recessive in Chinese hamster hybrid cells. J. Cell. Physiol. **106:**41–47.
26. **Huang, P., M. Gautschi, W. Walter, S. Rospert, and E. A. Craig.** 2005. The Hsp70 Ssz1 modulates the function of the ribosome-associated J-protein Zuo1. Nat. Struct. Mol. Biol. **12:**497–504.
27. **Hundley, H., et al.** 2002. The in vivo function of the ribosome-associated Hsp70, Ssz1, does not require its putative peptide-binding domain. Proc. Natl. Acad. Sci. U. S. A. **99:**4203–4208.
28. **Hundley, H. A., W. Walter, S. Bairstow, and E. A. Craig.** 2005. Human Mpp11 J. protein: ribosome-tethered molecular chaperones are ubiquitous. Science **308:**1032–1034.
29. **Inoue, T., W. Shoji, and M. Obinata.** 2000. MIDA1 is a sequence specific DNA binding protein with novel DNA binding properties. Genes Cells **5:**699–709.
30. **Inoue, T., W. Shoji, and M. Obinata.** 1999. MIDA1, an Id-associating protein, has two distinct DNA binding activities that are converted by the association with Id1: a novel function of Id protein. Biochem. Biophys. Res. Commun. **266:**147–151.
31. **Ishihara, K., K. Yasuda, and T. Hatayama.** 1999. Molecular cloning, expression and localization of human 105 kDa heat shock protein, hsp105. Biochim. Biophys. Acta **1444:**138–142.
32. **Kabani, M., and C. N. Martineau.** 2008. Multiple hsp70 isoforms in the eukaryotic cytosol: mere redundancy or functional specificity? Curr. Genomics **9:**338–348.
33. **Kampinga, H. H., et al.** 2009. Guidelines for the nomenclature of the human heat shock proteins. Cell Stress Chaperones **14:**105–111.
34. **Kim, S. Y., and E. A. Craig.** 2005. Broad sensitivity of Saccharomyces cerevisiae lacking ribosome-associated chaperone Ssb or Zuo1 to cations, including aminoglycosides. Eukaryot. Cell **4:**82–89.
35. **Kotler-Brajtburg, J., G. Medoff, G. S. Kobayashi, and D. Schlessinger.** 1977. Sensitivity to amphotericin B and the cholesterol: phospholipid molar ratios of 3T3, L, BHK and HeLa cells. Biochem. Pharmacol. **26:**705–710.
36. **Kramer, G., D. Boehringer, N. Ban, and B. Bukau.** 2009. The ribosome as a platform for co-translational processing, folding and targeting of newly synthesized proteins. Nat. Struct. Mol. Biol. **16:**589–597.
37. **Matsumoto-Taniura, N., F. Pirollet, R. Monroe, L. Gerace, and J. M. Westendorf.** 1996. Identification of novel M phase phosphoproteins by expression cloning. Mol. Biol. Cell **7:**1455–1469.
38. **Mayer, M. P., and B. Bukau.** 2005. Hsp70 chaperones: cellular functions and molecular mechanism. Cell. Mol. Life Sci. **62:**670–684.
39. **Meyer, A. E., N. J. Hung, P. Yang, A. W. Johnson, and E. A. Craig.** 2007. The specialized cytosolic J-protein, Jjj1, functions in 60S ribosomal subunit biogenesis. Proc. Natl. Acad. Sci. U. S. A. **104:**1558–1563.
40. **Miller, S. M., and D. L. Kirk.** 1999. glsA, a Volvox gene required for asymmetric division and germ cell specification, encodes a chaperone-like protein. Development **126:**649–658.
41. **O'Brien, M. C., K. M. Flaherty, and D. B. McKay.** 1996. Lysine 71 of the chaperone protein Hsc70 is essential for ATP hydrolysis. J. Biol. Chem. **271:**15874–15878.
42. **Okada, H., et al.** 2001. Immunization with an antigen identified by cytokine tumor vaccine-assisted SEREX (CAS) suppressed growth of the rat 9L glioma in vivo. Cancer Res. **61:**2625–2631.
43. **Otto, H., et al.** 2005. The chaperones MPP11 and Hsp70L1 form the mammalian ribosome-associated complex. Proc. Natl. Acad. Sci. U. S. A. **102:**10064–10069.
44. **Pappas, V., and S. M. Miller.** 2009. Functional analysis of the Volvox carteri asymmetric division protein GlsA. Mech. Dev. **126:**842–851.
45. **Peisker, K., et al.** 2008. Ribosome-associated complex binds to ribosomes in close proximity of Rpl31 at the exit of the polypeptide tunnel in yeast. Mol. Biol. Cell **19:**5279–5288.
46. **Peisker, K., M. Chiabudini, and S. Rospert.** 2010. The ribosome-bound Hsp70 homolog Ssb of Saccharomyces cerevisiae. Biochim. Biophys. Acta **1803:**662–672.
47. **Pfund, C., P. Huang, N. Lopez-Hoyo, and E. A. Craig.** 2001. Divergent functional properties of the ribosome-associated molecular chaperone Ssb compared with other Hsp70s. Mol. Biol. Cell **12:**3773–3782.
48. **Rakwalska, M., and S. Rospert.** 2004. The ribosome-bound chaperones RAC and Ssb1/2p are required for accurate translation in Saccharomyces cerevisiae. Mol. Cell. Biol. **24:**9186–9197.
49. **Raue, U., S. Oellerer, and S. Rospert.** 2007. Association of protein biogenesis factors at the yeast ribosomal tunnel exit is affected by the translational status and nascent polypeptide sequence. J. Biol. Chem. **282:**7809–7816.
50. **Raviol, H., H. Sadlish, F. Rodriguez, M. P. Mayer, and B. Bukau.** 2006. Chaperone network in the yeast cytosol: Hsp110 is revealed as an Hsp70 nucleotide exchange factor. EMBO J. **25:**2510–2518.
51. **Resto, V. A., et al.** 2000. A putative oncogenic role for MPP11 in head and neck squamous cell cancer. Cancer Res. **60:**5529–5535.
52. **Richly, H., et al.** 2010. Transcriptional activation of polycomb-repressed genes by ZRF1. Nature **468:**1124–1128.
53. **Rospert, S., M. Gautschi, M. Rakwalska, and U. Raue.** 2005. Ribosome-bound proteins acting on newly synthesized polypeptide chains, p. 429–458. *In* J. Buchner and T. Kiefhaber (ed.), Protein folding handbook, vol. II.1. Wiley-VCH Verlag GmbH & Co. KGaA, Weinheim, Germany.
54. **Rospert, S., M. Rakwalska, and Y. Dubaquié.** 2005. Polypeptide chain termination and stop codon readthrough on eukaryotic ribosomes. Rev. Physiol. Biochem. Pharmacol. **155:**1–30.
55. **Sambrook, J., and D. W. Russell.** 2001. Molecular cloning: a laboratory manual, vol. 2, p. 16.14–16.20. Cold Spring Harbor Laboratory Press, Cold Spring Harbor, NY.
56. **Schägger, H., and G. von Jagow.** 1987. Tricine-sodium dodecyl sulfate-polyacrylamide gel electrophoresis for the separation of proteins in the range from 1 to 100 kDa. Anal. Biochem. **166:**368–379.
57. **Shaner, L., R. Sousa, and K. A. Morano.** 2006. Characterization of Hsp70 binding and nucleotide exchange by the yeast Hsp110 chaperone Sse1. Biochemistry **45:**15075–15084.
58. **Shaner, L., A. Trott, J. L. Goeckeler, J. L. Brodsky, and K. A. Morano.** 2004. The function of the yeast molecular chaperone Sse1 is mechanistically distinct from the closely related hsp70 family. J. Biol. Chem. **279:**21992–22001.
59. **Sherman, F.** 1991. Getting started with yeast. Methods Enzymol. **194:**3–21.
60. **Shoji, W., T. Inoue, T. Yamamoto, and M. Obinata.** 1995. MIDA1, a protein associated with Id, regulates cell growth. J. Biol. Chem. **270:**24818–24825.
61. **Tavaria, M., T. Gabriele, I. Kola, and R. L. Anderson.** 1996. A hitchhiker's guide to the human Hsp70 family. Cell Stress Chaperones **1:**23–28.
62. **Theyssen, H., H. P. Schuster, L. Packschies, B. Bukau, and J. Reinstein.** 1996. The second step of ATP binding to DnaK induces peptide release. J. Mol. Biol. **263:**657–670.
63. **Thulasiraman, V., C. F. Yang, and J. Frydman.** 1999. In vivo newly translated polypeptides are sequestered in a protected folding environment. EMBO J. **18:**85–95.

64. **Tsukahara, F., and Y. Maru.** 2004. Identification of novel nuclear export and nuclear localization-related signals in human heat shock cognate protein 70. J. Biol. Chem. **279:**8867–8872.
65. **van de Wetering, M., et al.** 2003. Specific inhibition of gene expression using a stably integrated, inducible small-interfering-RNA vector. EMBO Rep. **4:**609–615.
66. **von Plehwe, U., et al.** 2009. The Hsp70 homolog Ssb is essential for glucose sensing via the SNF1 kinase network. Genes Dev. **23:**2102–2115.
67. **Wilbanks, S. M., C. DeLuca-Flaherty, and D. B. McKay.** 1994. Structural basis of the 70-kilodalton heat shock cognate protein ATP hydrolytic activity. I. Kinetic analyses of active site mutants. J. Biol. Chem. **269:**12893–12898.
68. **Xu, H., I. Y. Cheung, H. F. Guo, and N. K. Cheung.** 2009. MicroRNA miR-29 modulates expression of immunoinhibitory molecule B7-H3: potential implications for immune based therapy of human solid tumors. Cancer Res. **69:**6275–6281.
69. **Yaffe, M. P.** 1991. Analysis of mitochondrial function and assembly. Methods Enzymol. **194:**627–643.
70. **Yan, W., et al.** 1998. Zuotin, a ribosome-associated DnaJ molecular chaperone. EMBO J. **17:**4809–4817.
71. **Yoshida, M., T. Inoue, W. Shoji, S. Ikawa, and M. Obinata.** 2004. Reporter gene stimulation by MIDA1 through its DnaJ homology region. Biochem. Biophys. Res. Commun. **324:**326–332.